ISSN 0023-1584, Kinetics and Catalysis, 2009, Vol. 50, No. 1, pp. 111–121. © Pleiades Publishing, Ltd., 2009.
Original Russian Text © V.A. Matyshak, L.A. Berezina, O.N. Sil'chenkova, V.F. Tret'yakov, G.I. Lin, A.Ya. Rozovskii, 2009, published in Kinetika i Kataliz, 2009, Vol. 50, No. 1, pp. 120–131.

Properties of Surface Compounds in Methanol Conversion on γ-Al_2O_3: Data of In Situ IR Spectroscopy

V. A. Matyshak[a], L. A. Berezina[a], O. N. Sil'chenkova[a], V. F. Tret'yakov[b], G. I. Lin[b], and A. Ya. Rozovskii[b†]

[a] *Semenov Institute of Chemical Physics, Russian Academy of Sciences, Moscow, 119991 Russia*
[b] *Topchiev Institute of Petrochemical Synthesis, Russian Academy of Sciences, Moscow, 119991 Russia*
e-mail: matyshak@polymer.chph.ras.ru

Received July 18, 2007

Abstract—In situ IR spectroscopic studies show that a formate, an aldehyde-like complex, and bridging and linear methoxy groups exist on the alumina surface involved in methanol conversion. In the absence of methanol in the gas phase, the interaction between two bridging methoxy groups yields dimethyl ether in the gas phase. When methanol is present in the gas phase, it interacts with methoxy groups on the surface. This reaction makes the main contribution to the formation of dimethyl ether. The linear methoxy group undergoes conversion via several routes. The main route is desorption with methanol formation in the gas phase, and no more than 10% of the linear methoxy groups are converted into formate and aldehyde, which are CO_2 sources in the gas phase. In the absence of methanol in the gas phase, the conversion rate of the methoxy groups is independent of the presence of water and oxygen. A scheme of the surface reactions is suggested to explain the conversion of the methoxy groups.

DOI: 10.1134/S0023158409010157

INTRODUCTION

Methanol is among the key reactants in the syntheses of various compounds. The main routes of methanol conversion are the syntheses of dimethyl ether (DME) [1–3], methyl formate [4], formaldehyde [5], and hydrocarbons (motor fuels). In recent years, increasing attention has been given to the preparation of H_2-containing gas mixtures from methanol. This interest is mainly due to the development of fuel cells using hydrogen.

Copper-containing systems [6, 7] and catalysts containing noble metals [8, 9] are viewed as the most active catalysts for the preparation of hydrogen-containing mixtures from methanol. Along with the development of new catalytic systems, there has been considerable attention to the commercial catalyst SNM-1 for methanol synthesis ($CuO/ZnO/Al_2O_3$), which is also active in the preparation of hydrogen-containing gas mixtures from methanol. This catalytic system was chosen for studying the mechanism of catalytic methanol conversion. Since SNM-1 is a complicated three-component system, we chose to examine a series of catalysts with increasingly complex compositions: γ-Al_2O_3 $\longrightarrow$ Cu/γ-Al_2O_3 $\longrightarrow$ $CuO/ZnO/Al_2O_3$. Here, we report methanol conversion on γ-Al_2O_3.

The methoxy group $–O–CH_3$ is often regarded as a possible intermediate in methanol conversion on oxide systems [15–22]. In particular, the interaction of two methoxy groups is assumed to produce DME (see, e.g., [10]) and formaldehyde is assumed to result from the interaction between the methoxy group and oxygen [11, 12]. Formate complexes [13] and mixed complexes containing two methoxy groups and a surface hydroxyl group [14] are also considered to be intermediates in the methanol conversion reactions.

The complexes resulting from the interaction of methanol with the surface of oxide catalysts were characterized rather well [10–22]; however, the role of these complexes in the formation of reaction products remains unclear.

The main purpose of this work is to study the properties of the surface compounds and the routes of their conversion into products in methanol interaction with the γ-Al_2O_3 surface.

EXPERIMENTAL

We used γ-Al_2O_3 produced by Ryazan Petroleum Refinery [23]. The specific surface area of alumina was 190 m^2/g; the average particle radius was 55 μm; the total pore volume was 0.954 cm^3/g; and the Brønsted and Lewis acidities (measured by ammonia adsorption) were 4.8×10^{-7} and 1.5×10^{-7} mol/m^2, respectively.

The reactants were 4% methanol or DME + helium mixtures. Up to 3.3% oxygen was added to the methanol–helium mixture. Helium contained up to 0.2% oxygen as an impurity.

† Deceased.

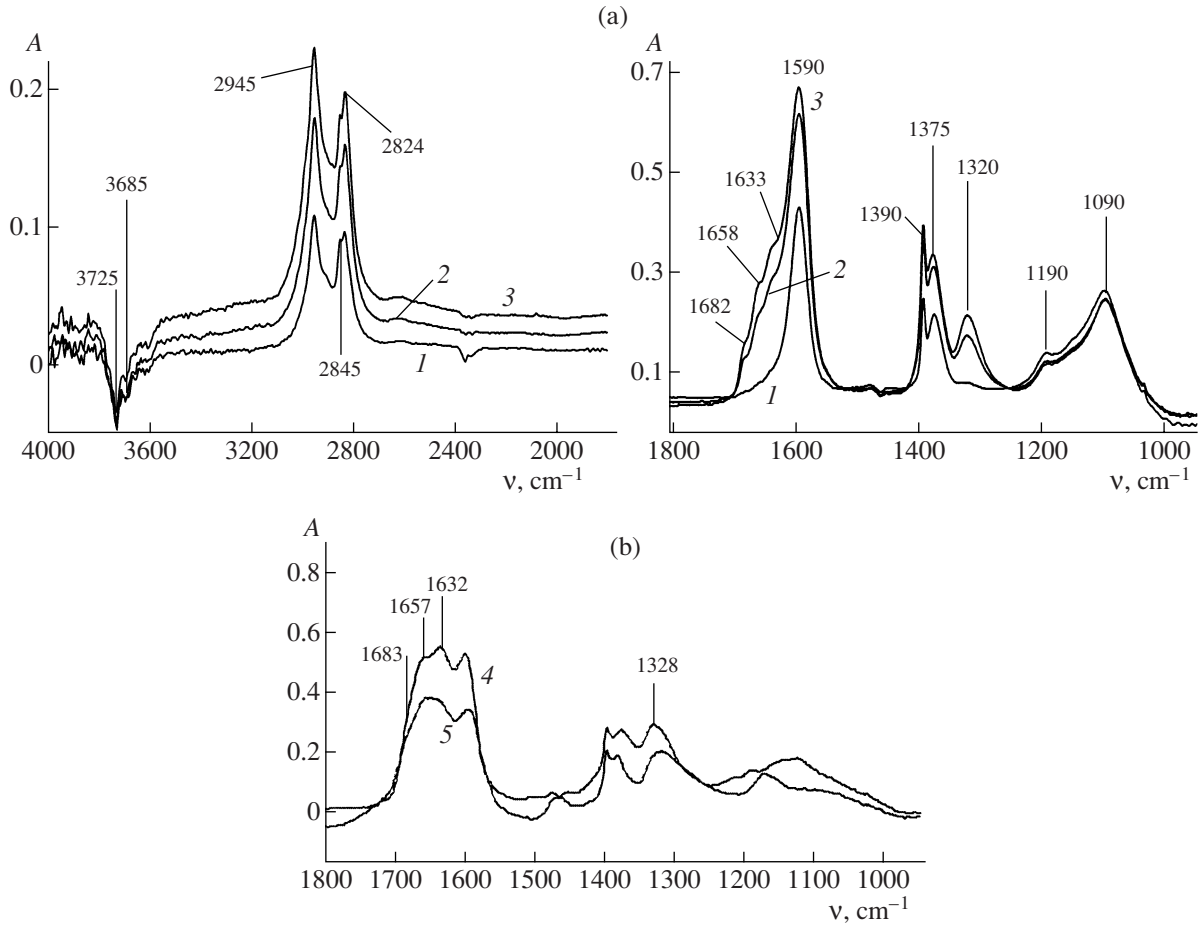

Fig. 1. IR spectra recorded for the reaction between methanol and oxygen on γ-Al_2O_3 at $T = 250$°C: (a) (*1*) 0% O_2, (*2*) 8.0% O_2, and (*3*) 12.0% O_2 (the spectrum of the initial γ-Al_2O_3 was subtracted from the spectra); (b) spectra of adsorbed (*4*) paraform and (*5*) glycolaldehyde ($T = 220$°C).

Spectroscopic kinetic studies under methanol conversion conditions were carried out using a standard procedure [24]. The experimental setup included a Spectrum RX I FT-IR System spectrometer (Perkin Elmer) or a Bruker IFS-45 spectrometer (Bruker), a heated spectroscopic cell employed as a flow reactor ($V = 1$ cm^3) [24], a gas preparation unit, and a product and reactant analysis system. Absorption intensities in transmission spectra were measured in absorbance units (A). The number of scans was usually 64, and the spectral resolution was 4 cm^{-1}.

A sample (20–30 mg pellet with a surface area of 2 cm^2) was placed in the cell, which simultaneously served as a flow catalytic reactor. Before measurements, the sample was conditioned in a flowing inert gas (He) at 450°C for 1 h and was cooled to the preset temperature. Next, the reaction mixture flow (30 ml/min) was switched on.

Unsteady-state spectroscopic kinetic studies included simultaneous measurements of the surface compound concentration by in situ IR spectroscopy and of the product formation rate by chromatography during the establishment of the steady-state kinetics of methanol conversion or upon the removal of methanol from the reaction mixture flow.

The concentrations of the reactants and reaction products were measured using a Model 3700 chromatograph (Khromatograf Plant, Moscow) with heated pipelines. The carrier gas was helium. DME, methanol, and methane were analyzed using a column packed with Porapak Q and a flame-ionization detector. Carbon monoxide, H_2, and CO_2 were analyzed using columns packed with molecular sieve 5A and Porapak Q and a thermal-conductivity detector.

RESULTS

Steady-State Measurements

The difference IR spectra measured under the methanol conversion conditions (4% methanol + He) on the γ-Al_2O_3 surface in the presence or absence of oxygen at $T = 250$°C are shown in Fig. 1a. The spectra contain absorption bands at 1682, 1658, 1633, 1590, 1390, 1375, 1320, 1190, 1150, and 1090 cm^{-1}. The 2800–

3000 cm^{-1} region exhibits intense absorption bands at 2945, 2845, and 2824 cm^{-1} due to C–H stretching vibrations. Negative peaks at 3685 and 3725 cm^{-1} are observed in the region of the stretching vibrations of surface OH groups. This indicates that the hydroxyl groups are consumed during the interaction of methanol with the surface.

Paraform and glycolaldehyde adsorption onto the sample was carried out to refine the assignment of the absorption bands at 1700–1500 cm^{-1}. The corresponding spectra are presented in Fig. 1b.

The plots of the concentrations of methanol and the products of its conversion versus experimental temperature are shown in Fig. 2a (4% MeOH in He was used as the reaction mixture). Water and DMA were identified among the reaction products. Above 300°C, the formation of H_2, CO, CO_2, and CH_4 takes place and their total concentration does not exceed ~0.6%.

The temperature dependences of the absorption band intensities in the IR spectra recorded under the same experimental conditions are presented in Fig. 2b. According to the temperature dependence of adsorption intensity, these bands can be divided into four groups (Figs. 1a, 2b) so that the ratio of their intensities is temperature-independent within one group. The first group includes the absorption bands at 1590, 1390, 1375, and 2905 cm^{-1}; the second group consists of the bands at 1633, 1658, 1682, 1320, and 2890 cm^{-1}; the third group, of the bands at 1090, 2945, and 2845 cm^{-1}; and the fourth, of the bands at 1190, 1150, and 2825 cm^{-1}. These groups are assigned to the surface formate complex, the surface aldehyde, the bridging methoxy group, and the linear methoxy group, respectively. This assignment will be substantiated below.

In further analysis, the relative concentrations of these surface complexes were estimated from the absorption intensities at 1590 cm^{-1} (formate), 1320 cm^{-1} (aldehyde), 1090 cm^{-1} (bridging methoxy group), and 1190 cm^{-1} (linear methoxy group).

Note that formate has a high thermal stability and its absorption bands persist in the spectra even after heating the sample to 400°C [12].

To confirm the assignment of IR bands to the aldehyde complex, we carried out the adsorption of formaldehyde and glycolaldehyde (Fig. 1b, spectra *4*, *5*) and the deconvolution of the corresponding spectra at 1550–1700 cm^{-1} using standard programs under the assumption of the Lorentzian shape of the absorption bands (Fig. 3).

Unsteady-State Measurements

The changes in IR absorption intensities and the product composition in the gas phase were monitored after the steady-state values of the surface compound concentrations in the 4% methanol + helium flow were established and methanol was excluded from the reaction mixture. According to chromatographic data, the desorption products contain DME, methanol, and minor amounts of CO_2 (less than 0.1 vol %). The absorption spectra exhibit absorption bands of the formate, aldehyde, and the bridging and linear methoxy groups.

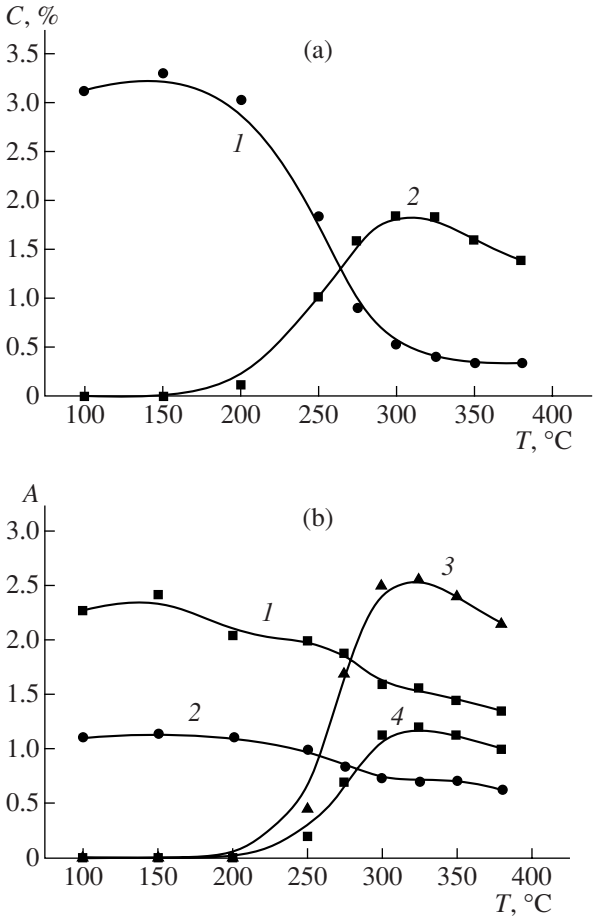

Fig. 2. Temperature dependences of (a) the substance concentrations in the gas phase and (b) the amounts of surface compounds according to IR spectroscopic data for the conversion of 4% methanol in helium: (a) (*1*) CH_3OH and (*2*) DME; (b) (*1*) 1090, (*2*) 1190, (*3*) 1590, and (*4*) 1320 cm^{-1}.

The time dependences of the intensities of the methoxy group absorption bands (1090, 1190 cm^{-1}) at different temperatures are presented in Fig. 4. These kinetic profiles make it possible to determine the apparent rate constants, the reaction order of the consumption of the surface complex, and the activation energy.

Typical results of kinetic data processing are presented in Fig. 5. The equation describing the evolution of the concentration of bridging methoxy groups is second-order, whereas the order of the equation that describes the variation of the linear methoxy group concentration is close to unity. The rate constants calculated from the slopes of the corresponding straight lines (derived from IR spectroscopic data) are listed in Table 1.

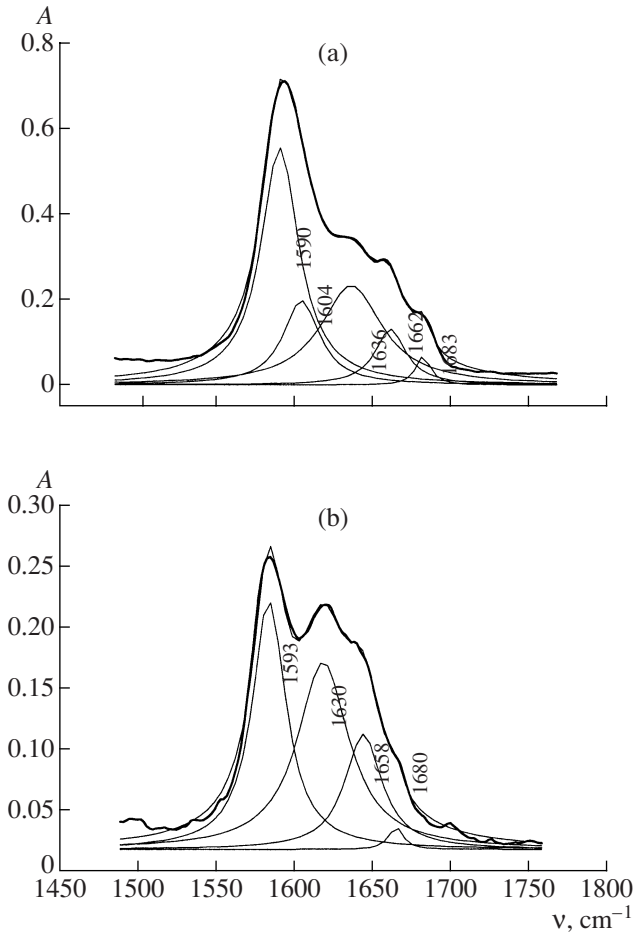

Fig. 3. IR spectrum the 1550–1700 cm^{-1} range and the results of its deconvolution: (a) after methanol adsorption and (b) after paraform adsorption. The thick line is the observed spectrum.

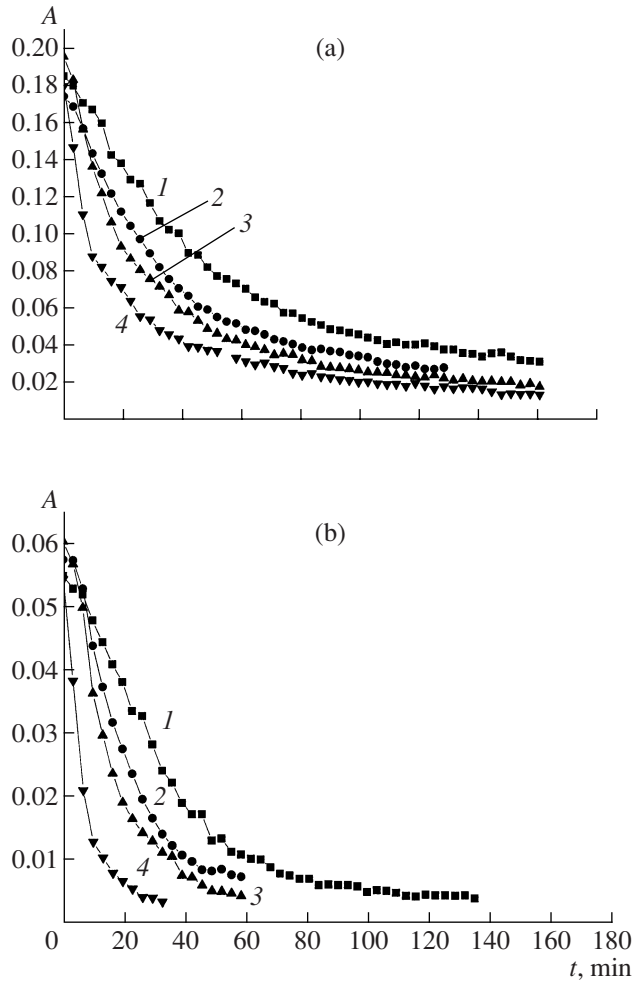

Fig. 4. Time evolution of the intensities of the absorption bands at (a) 1090 and (b) 1190 cm^{-1}. Desorption in flowing helium at T = (*1*) 180, (*2*) 210, (*3*) 240, and (*4*) 270°C.

The corresponding activation energies were determined from the temperature dependences of the rate constants: E_a^{1090} = 25 kJ/mol and E_a^{1190} = 30 kJ/mol.

The kinetic curves of formate formation on the surface at low temperatures fit the first-order equation well. The rate constants at low temperatures and the initial rates of formate formation (determined at the moment of methanol exclusion from the reaction mixture) throughout the temperature interval examined are given in Table 1. The activation energy determined from the initial rates is 80 kJ/mol, and that determined from the rate constants is 13 kJ/mol. These activation energy data indicate that the formate is both formed and consumed at ≥240°C.

The formation of the aldehyde complex (1320 cm^{-1}) on the Al_2O_3 surface during desorption into the helium flow occurs only at ≥240°C. It is interesting that the temperature at which the aldehyde begins to form is close to the temperature at which the formate complex begins to disappear (Fig. 6). The curves are S-like and indicate an induction period, which shortens as the temperature is raised.

Influence of oxygen on the conversion of the surface complexes. An increase in the oxygen concentration in helium from 0 to 3.3% does not exert any significant effect on the rate of methoxy group consumption (Table 2).

When oxygen is introduced into the gas flow, the formate formation rate increases, and the steady-state intensity of the absorption band of the formate is noticeably higher than was observed in the absence of oxygen in the mixture. The formate formation rate constants at different oxygen concentrations at 240°C are presented in Table 2. At higher temperatures, the formate complex forms as early as methanol adsorption takes place. This is indicated by the presence of absorption bands from this complex in the spectra recorded during adsorption.

The introduction of oxygen has a substantial effect on the character of the time variation of the aldehyde

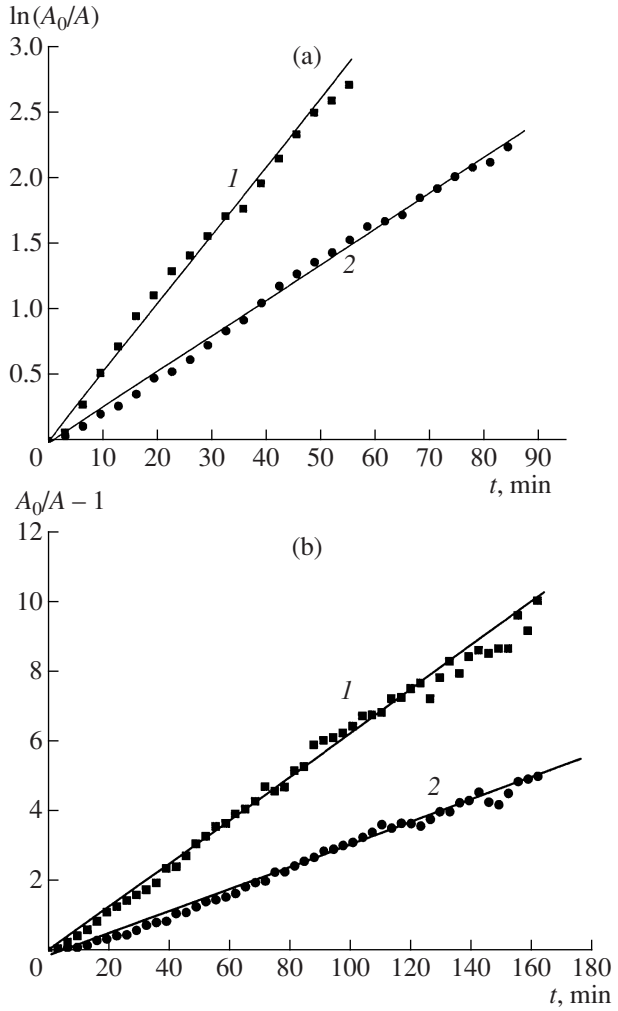

Fig. 5. Example of kinetic data fitting to (a) a first-order equation (absorption band at 1190 cm^{-1}) and (b) a second-order equation (absorption band at 1090 cm^{-1}). Desorption in flowing helium at T = (*1*) 240 and (*2*) 180°C.

complex concentration (1320 cm^{-1}). At 240°C, the intensity versus time plots are S-like at all oxygen concentrations and the induction period shortens with an increase in the oxygen concentration (Fig. 7). It is of interest that the intensity maximum of the absorption bands of the aldehyde complex coincides in time with the almost complete absence of the absorption band at 1190 cm^{-1} from the spectra (Fig. 7).

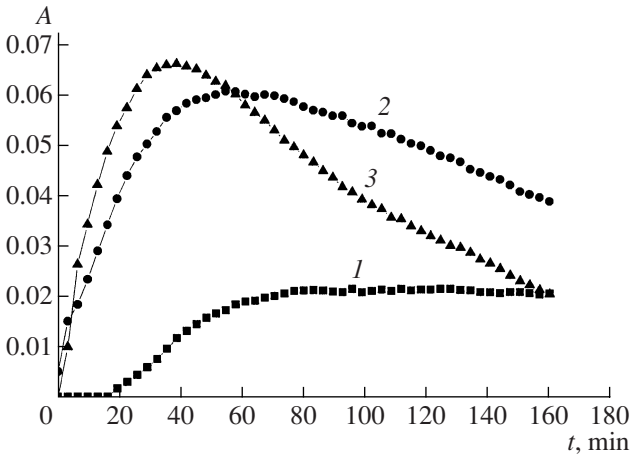

Fig. 6. Time evolution of the intensity of the absorption band at 1320 cm^{-1}. Desorption in flowing helium at T = (*1*) 240, (*2*) 260, and (*3*) 270°C.

Influence of water on the conversion of the surface complexes. The presence of water vapor exerts no substantial effect on the character of the consumption of the bridging and linear methoxy groups or formate formation. The quantitative characteristics of methoxy group consumption and formate formation in the presence of water vapor are given in Table 3. The presence of water vapor in the helium mixture decreases the formate concentration on the γ-Al_2O_3 surface.

The aldehyde is formed on the surface only in a flow containing 0.6% H_2O. The time profile of the intensity of the absorption band at 1320 cm^{-1} is S-like. The introduction of water into helium extends the induction period (20 min without water against 30 min in the presence of 0.6% H_2O). No aldehyde forms in the presence of 3% water vapor in helium.

Table 1. Temperature dependences of the rate constants of methoxy group consumption and formate formation (desorption in flowing helium)

T, °C	k, min^{-1}		Formate formation (1590 cm^{-1})	
	linear (1190 cm^{-1}) n = 1	bridging* (1090 cm^{-1}) n = 2	k, min^{-1}	w_o, arb. units
180	0.0265	0.0302	0.0250	0.0003
210	0.0437	0.0417	0.0343	0.00194
240	0.0760	0.0609	0.0345	0.0042
260	0.0928	0.0579	–	0.0088
270	0.1008	0.0761	–	0.01

Note: n is the reaction order.

* The constants were determined from spectroscopic data in which the concentration was expressed in terms of dimensionless absorbance A.

Table 2. Dependences of the rate constants of methoxy group consumption and formate formation on the oxygen concentration in helium (T = 240°C)

Concentration of O_2, %	k, min^{-1}		
	linear (1190 cm^{-1}) n = 1	bridging* (1090 cm^{-1}) n = 2	formate (1590 cm^{-1}) n = 1
0	0.0760	0.0609	0.0345
1.0	0.0738	0.0714	0.0746
2.0	0.0687	0.0611	0.0620
3.3	0.0750	0.0625	0.0731

* The constants were determined from spectroscopic data in which the concentration was expressed in terms of dimensionless absorbance A.

Table 3. Dependences of the rate constants of methoxy group consumption and formate formation on the concentration of water vapor in helium (T = 240°C)

Concentration of H_2O, %	k, min^{-1}		
	linear (1190 cm^{-1}) n = 1	bridging (1090 cm^{-1}) n = 2	formate (1590 cm^{-1}) n = 1
0	0.0760	0.0609	0.0345
0.6	0.0614	0.0750	0.0338
3.0	0.0645	0.0693	0.0360

The intensity of the absorption bands of the OH groups increases during desorption of the surface compounds. Therefore, the OH groups form again via reactions occurring on the Al_2O_3 surface. The kinetics of methoxy group consumption and formate, aldehyde, and OH group formation (absorption band at 3725 cm^{-1}) during desorption are shown in Fig. 8. It can be seen that the changes in the intensity of the OH groups correlate with the changes in the bridging methoxy group concentration. However, it is most likely that the OH groups result from several surface reactions.

DISCUSSION

Assignment of IR Absorption Bands

The absorption bands at 1590, 1390, and 1375 cm^{-1} are assigned to vibrations in the surface formate complex (see, e.g., [15, 25–27]). Based on published data [15–17], the absorption bands at 1190–1090 cm^{-1} can be assigned to the ν(C–O) vibrations in the linear (1190 cm^{-1}) and bridging (1090 cm^{-1}) methoxy groups.

According to earlier studies [28, 29], the absorption bands at 1190 cm^{-1} are assigned to the $\delta(CH_3)$ vibrations in the bridging methoxy group. Our data show that the intensities of the absorption bands at 1190 and 1090 cm^{-1} in the steady- and unsteady-state experiments change differently. This proves that these bands are due to different surface methoxy groups. A detailed analysis of spectroscopic data (Fig. 1) (in particular, obtaining difference spectra so as to eliminate the absorption band at 1090 cm^{-1}) shows the presence of a low-intensity band at 1140–1150 cm^{-1}. The changes in its intensity in different experiments correlate with the changes in the intensity of the absorption band at 1190 cm^{-1}. Therefore, the weak absorption band is due to the $\delta(CH_3)$ vibrations in the linear methoxy group.

At least five vibrations are observed in the region of C–H stretching vibrations. An analysis of the changes in their intensity in the steady- and unsteady-state experiments versus the changes in the intensity of the absorption bands of other surface compounds made it possible to distinguish the absorption bands due to the bridging and linear methoxy groups and the formate and aldehyde complexes (Table 4).

The set of absorption bands at 1320 and 1608, 1633, 1658, and 1682 cm^{-1} (Figs. 1, 3) is assigned to vibrations in adsorbed formaldehyde. This inference is confirmed by the fact that similar IR spectra are observed for the high-temperature (220°C) adsorption of paraform and the adsorption of glycolaldehyde and methyl formate [12]. All these molecules can form the same fragments during adsorption. Paraform consists of formaldehyde molecules, glycolaldehyde can dissociate into two formaldehyde molecules during adsorption, and methyl formate dissociates into a formaldehyde molecule and the oxymethylene complex. In addition, similar results were obtained by the deconvolution of the composite absorption at 1550–1700 cm^{-1} (Fig. 3a) and the absorption in the same region observed after paraform adsorption (Fig. 3b). Note that complexes with a similar structure (η^2-H_2CO) are viewed as intermediates in methanol synthesis [33].

In other words, a set of aldehyde-like complexes containing a carbonyl bond and a C–H bond in CHO (1320 cm^{-1}) is observed on the surface in our case. The fact that the C=O frequency in these complexes is substantially lower than the same frequency in the formaldehyde and glycolaldehyde molecules (1740 cm^{-1}) means that the corresponding vibrations are actively involved in the formation of bonds with the surface. A decrease in the C=O frequency during formaldehyde adsorption was also observed in [30, 31]. The observation of a set of complexes differing in carbonyl vibration frequency is due to the presence of sites of different natures (such as phase heterogeneity and extralattice cations [32]) on the γ-Al_2O_3 surface. As compared to the carbonyl vibration frequency, the CHO vibration frequencies in these complexes are much less different. However, the absorption band at 1320 cm^{-1} is not single, as is indicated by its comparatively large half-width and by the position of its maximum changing within a narrow interval in different experiments.

The hydroxyl coverage of γ-Al_2O_3 has a complicated structure [34]. According to our data, hydroxyl

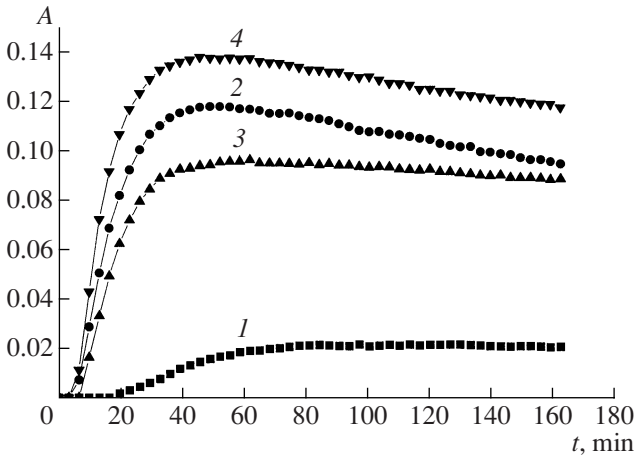

Fig. 7. Time evolution of the intensity of the absorption band at 1320 cm^{-1}. Desorption in flowing helium with an oxygen concentration of (*1*) 0, (*2*) 1, (*3*) 2, and (*4*) 3.3%; T = 240°C.

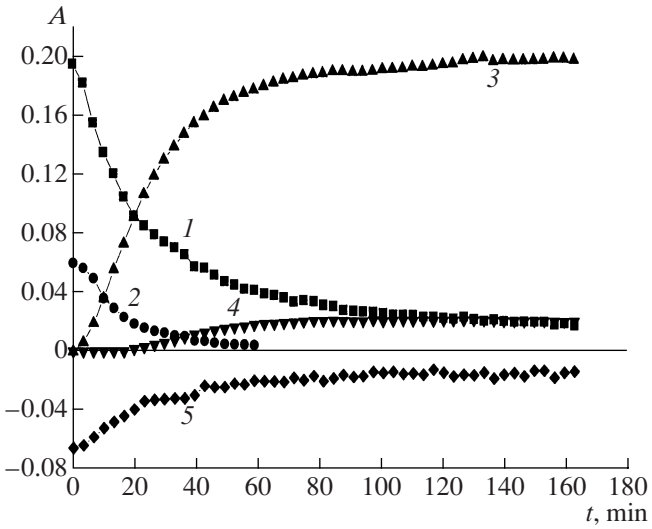

Fig. 8. Time evolution of the intensities of the absorption bands at (*1*) 1090, (*2*) 1190, (*3*) 1590, (*4*) 1320, and (*5*) 3725 cm^{-1} for desorption in flowing helium at T = 240°C.

groups of two types, with vibration frequencies of 3725 and 3685 cm^{-1}, participate in methanol adsorption. These frequencies correspond to the vibrations in the terminal and geminal hydroxyl groups, respectively [34].

The assignment of absorption bands observed under the reaction conditions to particular vibrations is shown in Table 4.

The formation of the methoxy groups via the interaction of the sample with methanol is accompanied by a decrease in the intensity of the absorption bands of the hydroxyl groups at 3725 and 3685 cm^{-1} (Fig. 1). Therefore, the methoxy groups form according to the classical scheme (via C–O bond cleavage in the alcohol molecule), involving acidic hydroxyl groups of the surface [15]: the formation of the linear methoxyl groups involves terminal hydroxyl groups, and the formation of bridging methoxyl groups involves geminal hydroxyls.

Conversion of the Surface Complexes

Kinetic data (Figs. 4, 5) show that the linear and bridging methoxy groups are consumed in radically different ways. The linear methoxy group is consumed according to a first-order equation; the bridging group, according to a second-order equation.

Bridging methoxy group. As determined by temperature-programmed desorption (TPD) [35, 36], the products of methanol desorption from γ-Al_2O_3 into the gas phase are methanol and DME (T_{des} = 225–525°C), H_2O (T_{des} = 225–625°C), CO and H_2 (T_{des} > 380°C), and CO_2 (T_{des} > 425°C). According to our data (Fig. 1), above 150°C the surface contains no adsorbed methanol (which is identifiable as intense absorption at 1030 cm^{-1} [15, 28]). This means that all of the desorption products result from the conversion of the surface methoxy groups. Therefore, the second-order rate law of the consumption of bridging methoxy groups (Fig. 5b) suggests that precisely this complex is the source of DME in the gas phase. The activation energy of bridging methoxy group conversion is 25 kJ/mol (Table 1). At the same time, the activation energy of

Table 4. Spectral manifestations of the surface complexes

Frequency, cm^{-1}	Assignment	Surface complex
1682 1658 1633 1608	ν(C=O)	Formaldehyde coordinated in the monodentate and bidentate modes
1320	δ(CH) in CHO	
2890	$\nu_{as}(CH_2)$	
1590	$\nu_{as}(COO^-)$	Formate
1390	$\nu_s(COO^-)$	
1375	δ(CH)	
2905	ν(CH)	
1190	ν(–O–C)	Linear methoxy group
1150	$\delta(CH_3)$	
2825	$\nu_s(CH_3)$	
1090	ν(>O–C)	Bridging methoxy group
2845	$\nu_s(CH_3)$	
2945	$\nu_{as}(CH_3)$	
3725	ν(–OH)	Hydroxyl group
3685	ν(>OH)	

DME formation measured for the same sample in the presence of methanol in the gas phase [12] is 40 kJ/mol. To explain the difference in activation energy, we estimated the rate of DME formation by the recombination of two methoxy groups at 240°C as

$$w_r = k\Theta_m\Theta_m,$$

where Θ_m is the methoxy group coverage of the surface and k is the rate constant of methoxy group consumption, which is 0.06 min^{-1} (Table 1). By converting the coverages into concentrations, we obtain $w_r = k^*N_mN_m$, where N_m is the number of methoxy groups in the sample and k^* is the rate constant of methoxy group consumption (its dimension corresponds to the second-order rate law). The N_m values are determined using the Lambert–Beer law: $N_m = DS/\varepsilon$, where D is the absorbance of the absorption band, ε is the extinction coefficient, and S is the geometric surface area of the sample.

The concentration of bridging methoxy groups on the surface at 240°C was estimated using the known extinction coefficients for vibrations [37]. It turned out that the number of bridging methoxy groups on the sample was 10^{19} (2.5×10^{14} complex/cm^2). In other words, for DME resulting from the interaction of two methoxy groups, the formation rate is 6×10^{17} molecule/min. The experimentally measured rate for the same sample at 240°C is 10^{19} molecule/min; therefore, the interaction between two methoxy groups is not the main route of DME formation. It is likely that the main route is the interaction between a methoxy group and a methanol molecule from the gas phase. This result is important evidence that DMF forms both by the reaction between two methoxy groups and by the interaction between a methoxy group and a methanol molecule from the gas phase, the latter reaction being the main route (see relevant discussion in [35, 38–45]).

According to TPD data and kinetic measurements [35, 46], the activation energy of DME formation on γ-Al_2O_3 is 90 ± 10 kJ/mol. The difference between this value and our data likely arises from the different natures of the surfaces of the γ-Al_2O_3 samples.

A decrease in the methoxy group concentration is accompanied by an increase in the concentration of surface OH groups (Fig. 8). The time profiles of the concentration of surface OH groups cannot be fitted to a first- or second-order equation. This is likely due to the fact that the hydroxyl groups form by several surface reactions with different kinetic parameters.

Influence of oxygen and water vapor on the conversion of the bridging methoxy group. The desorption of methoxy groups in a flow containing oxygen or water at different concentrations exerts no appreciable effect on the character and rate of the consumption of bridging methoxy groups (Tables 1–3). This is further evidence that the surface bridging methoxy groups are consumed in DME formation and that water and oxygen are not involved in this reaction and do not affect the consumption rate of bridging methoxy groups.

Linear methoxy group. The formate and aldehyde complexes appear on the surface during the consumption of the methoxy groups. The time dependence of the intensity of the aldehyde complex absorption band at experimental temperatures higher than 240°C is a curve with a maximum. The absorption maximum of the aldehyde complex coincides in time with the almost complete absence of the absorption band at 1190 cm^{-1} (Figs. 4, 6, 7). Since the aldehyde is both formed and consumed on the surface, this situation is possible if the aldehyde results from the conversion of the linear methoxy group.

Both the formate complex formation kinetics and the linear methoxy group consumption kinetics (Fig. 5a) are fittable to a first-order equation. At 180°C, when the aldehyde complex has not yet been formed, the rate constant of linear methoxy group consumption is equal to that of formate formation (Table 1). This observation along with the fact that the absorption intensity of the formate complex decreases when the linear methoxy group is missing from the spectrum (Fig. 4b) indicates that it is this kind of methoxy group that is the source of the formate complex on the γ-Al_2O_3 surface. The formate complex formation kinetics in methanol conversion on zinc oxide was also fitted to a first-order equation [47]. The activation energy was calculated from rate constant and initial $HCOO^-$ formation rates to be 85 kJ/mol. The activation energy determined by us (Table 1) is 80 kJ/mol.

According to our data (Fig. 7), the presence of oxygen exerts a substantial effect on the rate of aldehyde formation. This means that oxygen rather than the hydroxyl group participates in aldehyde formation. An indirect confirmation of this route is the increase in the hydroxyl group concentration on the surface (Fig. 8). The oxygen that is involved in aldehyde formation is activated on surface defects [12].

The aldehyde complex can turn into formate or a dioxymethylene complex [30, 48]. However, the onset temperature of formate formation is considerably lower than that of aldehyde formation (Fig. 6). In addition, the absorption bands of the dioxymethylene complex (~1000–1200, ~1400 cm^{-1} [30]) were not observed under any experimental conditions. This means that the conversion of the aldehyde complex into the formate or dioxymethylene complex does not occur on γ-Al_2O_3.

Some oxygen species is assumed to be involved in the formation of the formate [22, 39, 47, 49]. According to our data, the rate of formate accumulation indeed increases in the presence of oxygen (Table 2). At the same time, since no appreciable amount of hydrogen forms on γ-Al_2O_3, the route involving oxygen adsorbed in molecular form seems to be the most likely (the reaction involving oxygen atoms would yield hydrogen).

Formate and aldehyde complexes. The time profiles of the absorption band intensities for the aldehyde and formate complexes have an extremum (Fig. 6). This indicates that the resulting surface complexes undergo

further conversion. Several routes of the decomposition of the formate and aldehyde complexes are possible, depending on the process conditions [29, 45, 50, 51]. In our case, since oxygen affects the accumulation of these complexes on the surface and the products formed during the desorption of the surface compounds contain a small amount of CO_2 (<0.1 vol %) along with DME and methanol, the further conversion of the aldehyde complex is oxidation and that of the formate complex is a decomposition reaction yielding CO_2.

The above considerations and the fact that the rates of methoxy group conversion remain almost unchanged in the presence of water vapor and oxygen suggest the following scheme for the surface reactions responsible for methanol conversion on γ-Al_2O_3. The scheme also takes into account the participation of methanol from the gas phase in the formation of DME.

No.	Step
(I)	$CH_3OH_{(g)} + ZOH \longrightarrow CH_3OZ + H_2O_{(g)}$
(II)	$2CH_3OZ \longrightarrow (CH_3)_2O_{(g)} + ZO + Z$
(III)	$CH_3OH_{(g)} + CH_3OZ \longrightarrow (CH_3)_2O_{(g)} + ZOH$
(IIIa)	$H_2O_{(g)} + ZO + Z \longrightarrow 2ZOH$
	$2CH_3OH \longrightarrow (CH_3)_2O + H_2O$
(IV)	$Z^* + O_2 \longrightarrow ZO_2$
(V)	$ZO_2 + Z \longrightarrow 2ZO$
(VI)	$ZO_2 \longrightarrow Z + O_2$
(VI)I	$CH_3OH + ZOH \longrightarrow CH_3OZ + H_2O$
(VII)I	$CH_3OZ + ZO_2 \longrightarrow HCOOZ + H_2O + Z$
(IX)	$CH_3OZ + ZO \longrightarrow H_2COZ + ZOH$
(X)	$HCOOZ \longrightarrow CO_2 + ZH$
(XI)	$H_2COZ + ZO_2 \longrightarrow CO_2 + H_2O + 2Z$
(XII)	$CH_3OZ + ZH \longrightarrow CH_3OH + 2Z$
(XIII)	$H_2O + 2Z \longrightarrow ZOH + ZH$
(XIV)	$ZO + ZH \longrightarrow ZOH + Z$
	$2CH_3OH + 3O_2 \longrightarrow 4H_2O + 2CO_2$

This scheme accounts for the second-order rate law of the consumption of bridging methoxy groups in the absence of methanol in the gas phase (step (III)).

According to the scheme, the change in the concentration of linear methoxy groups is given by the following equation:

$$\frac{d(CH_3OZ)}{dt} = -Q_{CH_3OZ}(k_8Q_{ZO_2} + k_9Q_{ZO} + k_{12}Q_{ZH}), \quad (1)$$

where Q_i is the fraction of the surface occupied by the ith substance.

Since oxygen and water exert no effect on linear methoxy group conversion during desorption (Tables 1–3), the dominant step of linear methoxy group consumption is methoxy group desorption yielding methanol (step (XII)). Quantitative estimates confirming this conclusion will be presented below. According to these estimates, no more than 10% of the linear methoxy groups are transformed via routes (VIII) and (IX).

The existence of protons captured by a cationic vacancy on the γ-Al_2O_3 surface was reported by Dowden back in 1950 [52] and was confirmed by a later study [53]. The participation of a proton in methanol desorption ($CH_3OZ + HZ \longrightarrow CH_3OH_{(g)}$) was noted by Matsushima and White [39]. Therefore, the first-order rate law of linear methoxy group consumption can be explained by the fact that the number of cationic vacancies is not large and they are occupied by protons during methoxy group conversion, so Q_{ZH} is nearly constant.

An increase in the oxygen concentration in the helium flow increases the accumulation rate and the maximum concentration of both formate and aldehyde on the surface. However, the curves of accumulation of these complexes on the surface differ radically. The aldehyde accumulation curve indicates an induction period. In view of the fact that both complexes form from the same type of methoxy group, this difference means that the formation of these complexes involves oxygen of different natures. In the scheme, this fact is reflected as the presence of adsorbed oxygen atoms and molecules on the surface. For the aldehyde complex, the change in the concentration is expressed as

$$\frac{d(H_2COZ)}{dt} = k_9Q_{CH_3OZ}Q_{ZO} - k_{11}Q_{H_2COZ}Q_{ZO_2}. \quad (2)$$

With the corresponding values of the rate constants, the atomic oxygen coverage of the surface increases during desorption, whereas the molecular oxygen coverage decreases. This change in the coverages explains the existence of an induction period in the aldehyde complex accumulation curve. This assumption is confirmed by the data on desorption of surface compounds in the helium flow at 240°C (Fig. 9). Over the first 20 min, CO_2 formation in the gas phase takes place and no absorption bands of the aldehyde complex are observed in the IR spectrum. The time profile of the CO_2 concentration passes through a maximum. The disappearance of CO_2 from the gas phase coincides in time with the appearance of the absorption bands of the aldehyde complex (Fig. 9, curve *2*). This is likely due to the fact that the initial molecular oxygen coverage of the surface is high and the resulting aldehyde complex turns rapidly into CO_2 (step (XI)). This is the reason why the spectrum exhibits no absorption bands of the aldehyde complex. The molecular oxygen coverage of the surface decreases with time, whereas the atomic oxygen coverage increases, resulting in a decrease in the CO_2 concentration in the gas phase and in the appearance of the absorption bands of the aldehyde complex.

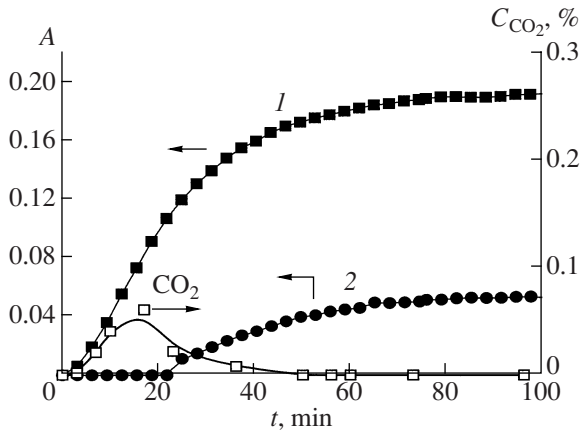

Fig. 9. Time dependences of the relative concentrations of the (*1*) formate complex and (*2*) aldehyde complex and the CO_2 in the gas phase for desorption in flowing helium at T = 240°C.

In a real situation, the possible sites of oxygen activation are surface defects of alumina. Many authors report that the surface of oxide systems has oxygen with unusual properties. In particular, it was reported [54, 55] that the surface of zeolite-containing catalysts (Tseokar-2) has strongly bound oxygen that stays on the surface upon high-temperature treatment in an inert atmosphere and can be removed only by the adsorption-assisted desorption involving H_2, H_2O, or CO_2. It should be taken into account that peroxide structures stable at high temperatures can exist on the surface. It is possibly these forms of oxygen that are responsible for the oxidation of the methoxy groups to formaldehyde. Note that the observed oxidation sites are very sensitive to the pretreatment of the sample. After Al_2O_3 conditioning in a gas flow containing a hydrocarbon (e.g., methanol), no absorption bands of the aldehyde are observed in the in situ spectrum. Their activity cannot be restored even by heating the sample in excess oxygen.

An increase in the rate of formate and aldehyde accumulation on the surface would be expected to be accompanied by an increase in the consumption rate of linear methoxy groups. In fact, this is not the case. Since the linear methoxy group undergoes conversion via several routes (see the scheme), the observed rate ratio can be explained by the fact that only a small proportion of the linear methoxy groups turns into formate and aldehyde. The concentrations of linear methoxy groups, formate, and aldehyde on the surface were estimated using known extinction coefficients of vibrations [37]. It turned out that the quantity of linear methoxy groups in the sample is 5×10^{18} complex/g (1.25×10^{14} complex/cm^2), the amount of aldehyde is 2×10^{17} complex/g (0.5×10^{13} complex/cm^2), and the amount of formate is 3×10^{17} complex/g (0.75×10^{13} complex/cm^2). These estimates suggest that no more than 10% of the linear methoxy groups are converted into formate and aldehyde. In other words, the terms pertaining to oxygen in Eq. (1) make a minor contribution to the consumption rate of linear methoxy groups.

When desorption is carried out in the presence of water, the rate constants of linear methoxy group consumption and formate formation do not change (Tables 1–3), and they are close to the values obtained for desorption in flowing helium. However, the maximum concentration of the formate complex decreases with an increase in the water concentration. This means that water does not affect the formation rate of the complex but blocks complex localization sites. Likewise, an increase in the water concentration in the helium flow decreases the maximum concentration of the aldehyde on the surface. Since an increase in the oxygen concentration shortens the induction period (Fig. 7), we can assume that water blocks specific oxygen adsorption sites or forces out oxygen from the surface [54, 55]. In the absence of oxygen adsorbed on these sites, the aldehyde stops forming.

Note that, in the absence of methanol in the gas phase, the interaction between two bridging methoxy groups affords DME. When present in the gas phase, methanol interacts with the bridging methoxy group on the surface, and this reaction makes the main contribution to the formation of DME.

The linear methoxy group is converted via several routes, namely, desorption yielding methanol in the gas phase and the formation of the surface formate and the aldehyde-like surface complex, which are sources of CO_2 in the gas phase.

ACKNOWLEDGMENTS

This work was supported by the Russian Foundation for Basic Research, grant no. 07-03-00373.

REFERENCES

1. Vishwanathan, M., Roh, H.-S., and Kim, J.-N., *Catal. Lett.*, 2004, vol. 96, p. 23.
2. Tleimat-Manzalji, R., Bianchi, D., and Pajonk, G.M., *React. Kinet. Catal. Lett.*, 1993, vol. 51, p. 29.
3. Bianchi, D., Chafik, T., Khalfallah, M., and Teichner, S.J., *Appl. Catal., A*, 1995, vol. 123, p. 89.
4. Sambeth, J.E., Juan, A., and Gambaro, L., *J. Mol. Catal. A: Chem.*, 1997, vol. 118, p. 283.
5. Sambeth, J.E., Centeno, M.A., and Paul, A., *J. Mol. Catal. A: Chem.*, 2000, vol. 161, p. 89.
6. Lindström, B., Pettersson, L., and Menon, P.G., *Appl. Catal., A*, 2002, vol. 234, p. 111.
7. Zhang, X. and Shi, P., *J. Mol. Catal. A: Chem.*, 2003, vol. 194, p. 99.
8. Iwasa, N., Mayanagi, T., and Ogawa, N., *Catal. Lett.*, 1998, vol. 54, p. 119.
9. Kapoor, M.P., Raj, A., and Matsumura, Y., *Microporous Mesoporous Mater*, 2001, vol. 44, no. 5, p. 565.

10. Schiffino, R.S. and Merril, R.P., *J. Phys. Chem.*, 1993, vol. 97, p. 6425.

11. Krylov, O.V. and Matyshak, V.A., *Promezhutochnye soedineniya v geterogennom katalize* (Intermediate Compounds in Heterogeneous Compounds), Moscow: Nauka, 1996.

12. Matyshak, V.A., Khomenko, T.I., Lin, G.I., Zavalishin, I.N., and Rozovskii, A.Ya., *Kinet. Katal.*, 1999, vol. 40, no. 2, p. 295 [*Kinet. Catal.* (Engl. Transl.), vol. 40, no. 2, p. 269].

13. Neophytides, S.G., Marchi, A.J., and Froment, G.F., *Appl. Catal., A*, 1992, vol. 86, p. 45.

14. Martin, K.A. and Zabransky, R.F., *Appl. Spectrosc.*, 1991, vol. 45, p. 68.

15. Davydov, A.A., *IK-spektroskopiya v khimii poverkhnosti okislov* (IR Spectroscopy Applied to the Chemistry of Oxide Surfaces), Novosibirsk: Nauka, 1984.

16. Daturi, M., Binet, C., Lavalley, J-C., Galtayries, A., and Spoken, R., *Phys. Chem. Chem. Phys.*, 1999, vol. 1, p. 5717.

17. Sidkon, A. and Nix, R.M., *J. Phys. Chem. B*, 1999, vol. 103, p. 6984.

18. Novakova, J., Kubelkova, L., and Dolysek, Z., *J. Catal.*, 1987, vol. 108, p. 208.

19. Lamotte, J., Moravek, V., Bensitel, M., and Lavalley, J.C., *React. Kinet. Catal. Lett.*, 1988, vol. 36, p. 113.

20. Knop-Gericke, A., Havecker, M., Schedel-Niedrig, Th., and Schlogl, R., *Top. Catal.*, 2000, vol. 10, p. 187.

21. Carley, A.P., Owens, A.W., Rajumon, M.K., Roberts, M.W., and Jackson, S.D., *Catal. Lett.*, 1996, vol. 37, p. 79.

22. Ueno, A., Onishi, T., and Tamaru, K., *Trans. Faraday Soc.*, 1971, vol. 67, p. 3585.

23. Matyshak, V.A., Khomenko, T.I., Bondareva, N.K., Panchishnyi, V.I., and Korchak, V.N., *Kinet. Katal.*, 1998, vol. 39, no. 1, p. 100 [*Kinet. Catal.* (Engl. Transl.), vol. 39, no. 1, p. 93].

24. Matyshak, V.A. and Krylov, O.V., *Catal. Today*, 1996, vol. 25, p. 1.

25. Millar, G.J., Rochester, C.H., and Waugh, K.C., *J. Chem. Soc., Faraday Trans.*, 1991, vol. 87, no. 17, p. 2795.

26. Millar, G.J., Rochester, C.H., and Waugh, K.C., *J. Chem. Soc., Faraday Trans.*, 1991, vol. 87, no. 17, p. 2785.

27. Burcham, L.J. and Wachs, I.E., *Catal. Today*, 1999, vol. 49, p. 467.

28. Busca, G., Rossi, P.F., Lorenzelli, V., Benaissa, M., Travert, J., and Lavalley, J.-C., *J. Phys. Chem.*, 1985, vol. 89, p. 5433.

29. Malakhova, I.V., Ermolaev, V.K., Danilova, I.G., Paukshtis, E.A., and Zolotarskii, I.A., *Kinet. Katal.*, 2003, vol. 44, no. 4, p. 587 [*Kinet. Catal.* (Engl. Transl.), vol. 44, no. 4, p. 536].

30. Busca, G., Lamotte, J., Lavalley, J.-C., and Lorenzelli, V., *J. Am. Chem. Soc.*, 1987, vol. 109, no. 11, p. 5197.

31. Clarke, D.B., Lee, D.-K., Sandoval, M.J., and Bell, A.T., *J. Catal.*, 1994, vol. 150, p. 81.

32. Kharlanov, A.A., *Cand. Sci. (Chem.) Dissertation*, Moscow: Moscow State Univ., 1995.

33. Ortelli, E.E., Weigel, J.M., and Wokaun, A., *Catal. Lett.*, 1998, vol. 54, p. 41.

34. Tsyganenko, A.A., *Doctoral (Phys.–Math.) Dissertation*, St. Petersburg: St. Petersburg State Univ., 2000.

35. Chen, B. and Falconer, J.L., *J. Catal.*, 1993, vol. 144, p. 214.

36. Clayborne, P.A., Nelson, T.C., and DeVore, T.C., *Appl. Catal., A*, 2004, vol. 257, p. 225.

37. Matyshak, V.A. and Krylov, O.V., *Kinet. Katal.*, 2002, vol. 43, no. 3, p. 422 [*Kinet. Catal.* (Engl. Transl.), vol. 43, no. 3, p. 391].

38. DeCanio, E.C., Nero, V.P., and Bruno, J.W., *J. Catal.*, 1992, vol. 135, p. 444.

39. Matsushima, T. and White, J., *J. Catal.*, 1976, vol. 44, p. 183.

40. Jain, J.R. and Pillai, C.N., *J. Catal.*, 1967, vol. 9, p. 322.

41. Padmanabhan, V.R. and Eastburn, F.J., *J. Catal.*, 1972, vol. 24, p. 88.

42. Knozinger, H., Kochloefl, K., and Meye, W., *J. Catal.*, 1973, vol. 28, p. 69.

43. Ivanov, S.I. and Makhlin, V.A., *Kinet. Katal.*, 1996, vol. 37, no. 6, p. 873 [*Kinet. Catal.* (Engl. Transl.), vol. 37, no. 6, p. 812].

44. Rozovskii, A.Ya., *Kinet. Katal.*, 2003, vol. 44, no. 3, p. 391 [*Kinet. Catal.* (Engl. Transl.), vol. 44, no. 3, p. 360].

45. Busca, G., *Catal. Today*, 1996, vol. 27, p. 457.

46. Spinicci, R., *Thermochim. Acta*, 1997, vol. 296, p. 87.

47. Herd, A.C., Onishi, T., and Tamaru, K., *Bull. Chem. Soc. Jpn.*, 1974, vol. 47, no. 3, p. 575.

48. Groff, R.P. and Marogue, W.H., *J. Catal.*, 1984, vol. 87, p. 461.

49. Yamashita, K., Naito, S., and Tamaru, K., *J. Catal.*, 1985, vol. 94, p. 535.

50. Amenomiya, Y., *J. Catal.*, 1979, vol. 57, p. 64.

51. Solymosi, F., Kiss, J., and Kovacs, I., *Surf. Sci.*, 1987, vol. 192, p. 47.

52. Dowden, D.A., *J.Chem. Soc*, 1950, nos. 1–2, p. 242.

53. Tsyganenko, A.A., Smirnov, K.S., Rzhevskiy, A.M., and Mardilovich, P.P., *Mater. Chem. Phys.*, 1990, vol. 26, no. 1, p. 35.

54. Vishnetskaya, M.V., Takhtarova, G.N., and Topchieva, K.V., *Kinet. Katal.*, 1985, vol. 26, no. 5, p. 1271.

55. Vishnetskaya, M.V., Takhtarova, G.N., and Topchieva, K.V., *Kinet. Katal.*, 1985, vol. 26, no. 5, p. 1272.